NANOCOMPOSITE ALLOY DESIGN FOR POWER ELECTRONIC APPLICATIONS.
IEEE Distinguished Lecture - 2013

Michael E. McHenry

Materials Science and Engineering Department
Carnegie Mellon University

The image cannot be displayed. Your computer may not have enough memory to open

Northrop Grumman

R. C. O'Handley (1942 – March 9, 2013) RIP
Beloved Teacher, author, researcher, husband and father.

IEEE Magnetics Society

- **IEEE Magnetics Society Home Page:** ***www.ieeemagnetics.org***
  - **3000 full members**
  - **300 student members**
- **The Society**
  - **Conference organization (INTERMAG, MMM, TMRC, etc.)**
  - **Student support for conferences**
  - **Large conference discounts for members**
  - **Graduate Student Summer Schools**
  - **Local chapter activities**
  - **Distinguished lectures**
- ***IEEE Transactions on Magnetics***
  - **~2000 peer reviewed pages each year**
  - **Electronic access to all *IEEE Transactions on Magnetics* papers**
- **Online applications for IEEE membership:** ***www.ieee.org/join***
  - **360,000 members**
  - **IEEE student membership IEEE full membership**

Outline

I. Introduction: Nanocomposites.
II. Energy Applications of Nanocomposites.
III. Issues for High Frequency Power Applications.
IV. Fe-rich Fe-Co-based Nanocomposite Alloys.
V. Co-rich Nanocomposites: Multiple Nanocrystal Phases.
IV. Conclusions.

Amorphous and Nanocrystalline Materials for Applications as Soft Magnets. **M. E. McHenry**, M. A. Willard and D. E. Laughlin; *Prog. Mat. Sci.*, **44**, 291-433, (1999).

What are Magnetic Nanocomposites?

Courtesy of J. Long

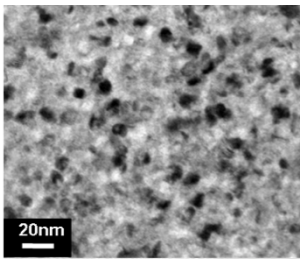

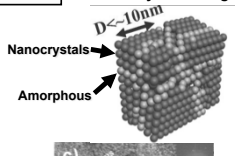

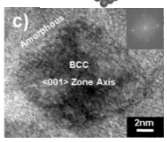

Ferromagnetic Nanocrystals Embedded in an Amorphous or Oxide Matrix:
Nanocrystals → High Induction
Matrix → Small Grain Size and Large Resistivity
Composite → Low Losses

Morphologies

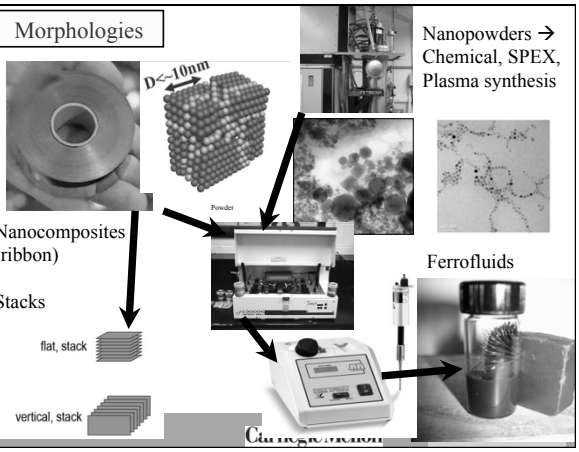

CoFe-SiOx Nanogranular Films Resonant Soft X-ray Scattering

U.S. DEPARTMENT OF ENERGY

BERKELEY LAB
LAWRENCE BERKELEY NATIONAL LABORATORY

Jeffrey Kortright. LBNL

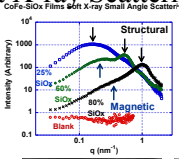

NETL-RUA
Regional University Alliance

Paul Ohodnicki
NETL

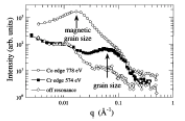

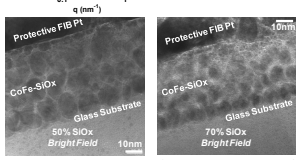

Resonant Soft X-ray Scattering Enables Quantiative Characterization of Microstructure in Magnetic Nanocomposites.

Introduction: Energy Applications of Nanocomposites

1. **Power Conversion**
2. **Electric Vehicles**
3. **Motors**
4. **Magnetocaloric Refrigeration and Heat Pumps**
5. **Reliable High Temperature Electronics Packaging**

S. Shen, P. R. Ohodnicki, S. J. Kernion, A. Leary, V. Keylin, J. Huth, & M. E. McHenry. *Nanocomposite Alloy Design For High Frequency Power Conversion Applications.* Energy Technology 2012: Carbon Dioxide Management and Other Technologies, 265 (2012). TMS Warrendale, PA.

Magnetic Materials for Energy Applications.

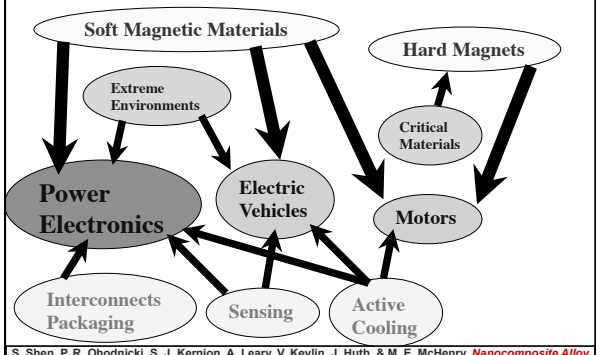

S. Shen, P. R. Ohodnicki, S. J. Kernion, A. Leary, V. Keylin, J. Huth, & M. E. McHenry. ***Nanocomposite Alloy Design For High Frequency Power Conversion Applications***. Energy Technology 2012: Carbon Dioxide Management and Other Technologies, 265 (2012). TMS Warrendale, PA.

Materials Paradigm for Power Transformation

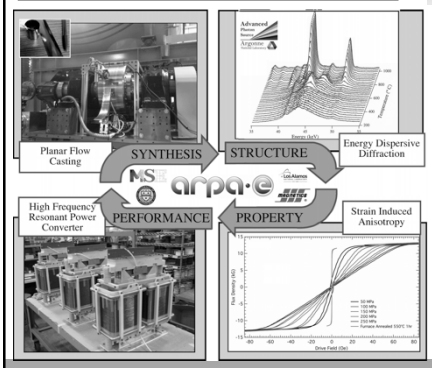

Wide Ribbons

Carnegie Mellon

Assisi 06/13/13

Target Electric Vehicle Applications

•J. Gover, A Tutorial on Hybrid Electric Vehicles: EV, HEV, PHEV and FCEV

Ribbons

J. Long, M.E. McHenry, D. Urciuoli, V. Keylin, J. Huth, & T. Salem, Nanocrystalline Material Development for High-Power Inductors. J. Appl. Phys. 103, 07E705-7 (2008). (http://dx.doi.org/10.1063/1.2829033).

Carnegie Mellon

Assisi 06/13/13

Materials Paradigm for Motor Applications

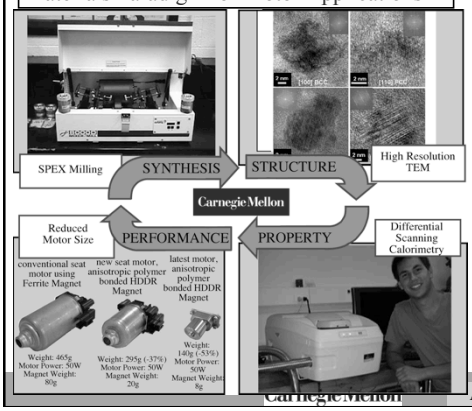

Flake

Carnegie Mellon

Assisi 06/13/13

Materials Paradigm for Magnetocaloric Cooling Applications

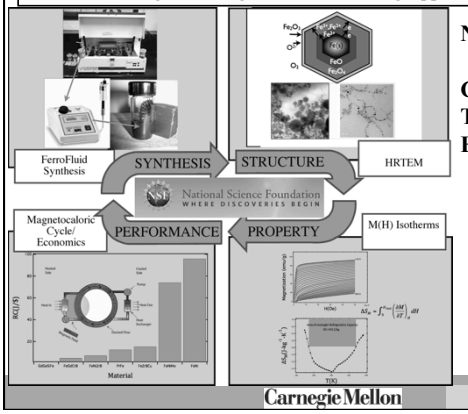

Nanopowder

Curie Temperature Engineering

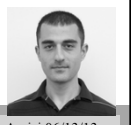

Nanofluidics – Thermal Transport

There is more to cooling than heat capacity! Thermal Conductivity is important.

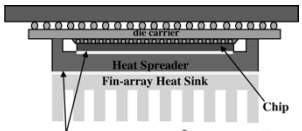

Thermal Interface Material

Fin Array

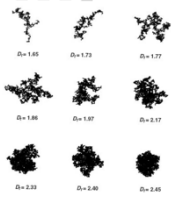

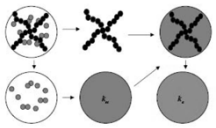

MNP chaining in an Applied Field.

Nanofluid Fin Array Heat Sinks.

SANDIA REPORT: SAND2010-3400 **Characterization and Modeling of Thermal Diffusion and Aggregation in Nanofluids** Patricia E. Gharagozloo and Kenneth E. Goodson

Materials Paradigm for High Temperature Interconnect Technologies

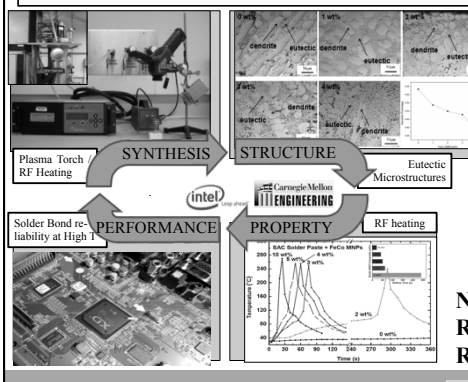

Nanopowder RF Heating Reliability

DOE Scattering Facilities

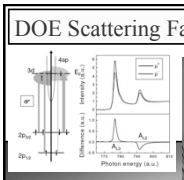

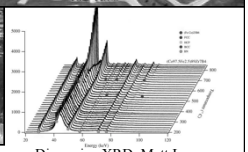

1. Argonne National Laboratory: High P T-dependent Energy Dispersive XRD: Matt Lucas
2. Lawrence Berkeley National Laboratory: Catherine Jenkins – XMCD, XMLD
3. Lawrence Berkeley National Laboratory: Jeffrey Kortright – Small Angle Scattering

Power Conversion Issues.

ADEPT FOA: Primary Technical Targets

Category	Voltage & Power	Efficiency	Switching Frequency	Size
Fully Integrated, Chip-scale power converters	>100V 10-50W	>93%	>5 MHz	Single-chip converters (including magnetics, capacitors, switches)
Package integrated power converters	>600V 3-10kW	>95%	>1 MHz	Multichip modules Package integrated converters
Lightweight, solid-state, medium voltage energy conversion	**13kV 1MW**	**>98%**	**>50 kHz**	**Transformers, converters.**

•Courtesy Rajeev Ram and Tim Heidel; ARPA-E

Near Equiatomic Fe-Co Alloys for Converters.

Army Research Laboratory

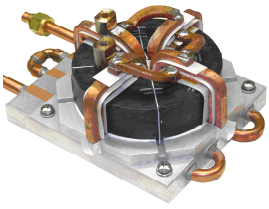

HTX-002 Inductor
Core Size - 4.23 ″ OD,
1.325 ″ ID, 1.095 ″ HT

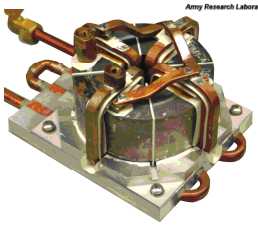

FINEMET Inductor
Core Size - 4.23″ OD,
1.325″ ID, 1.767″ HT

20 kW DC-DC Converter

J. Long, M. E. McHenry, D. P. Urciuoli, V. Keylin, J. Huth, and T. E. Salem. "Nanocrystalline material development for high-power inductors." *J. Appl. Phys.* **103**, (2008): 07E705.

Transformer Target: High f Nanocrystalline Transformers Are Over 150 Times Lighter And Significantly Smaller (At Same Power)

•HVCM Transformer

- 150 kV, 20 KHz
- 20 Amp RMS
- 1 MW Average (3) Present Use
- 450 LBS for 3
- 3 KW Loss At 2 MW
- "C" Core Design (Parallel Windings)

•Typical H.V. Transformers

- 100 kV, 60 Hz
- 20 Amp RMS
- 2 MW Average
- 35 Tons
- ~30 KW Loss

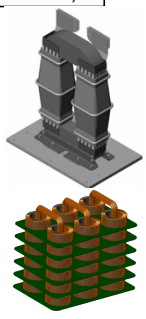

•Bill Reass - LANL

Los Alamos NATIONAL LABORATORY

NETL – Regional University Alliance

NETL – CMU Collaborations
Inductor Material Development w/ **Paul Ohodnicki**
Relevant for High Power, High Frequency Converters
(ARPA-E, Army)

NETL-RUA Strategic Growth Areas

Rare Earths and Critical Materials
DOE HUB Joint Proposal Submitted w/ Major Emphasis on Advanced Magnetic Materials (Soft, Hard, Magnetocaloric)

Grid Technologies Collaborative (GTC)
NETL Funded Seed Project Aimed at Development of Next Generation Power Converter
Greg Reed – University Pittsburgh

Metrics for Motivating Applications: Lossses.

$$P_{tot} = P_h + P_e + P_a$$

Hysteresis Losses $P_h = afB^2$ **Random anisotropy**

Eddy Current Losses $P_e = bf^2B^2$

$b = \frac{(\pi \cdot t)^2}{6 \cdot \rho}$ **Resistivity, Thickness**

Anomalous Losses

$P_a = e(f \cdot B)^{1.5}$

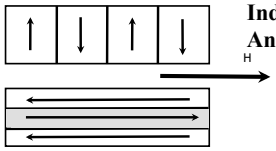

Induced Anisotropy

Scaling

What material properties are necessary for high frequency operation?

A., Leary, P. Ohodnicki, M. E. McHenry, Soft Magnetic Materials in High Frequency, High Power Conversion Applications; JOM, 2012.

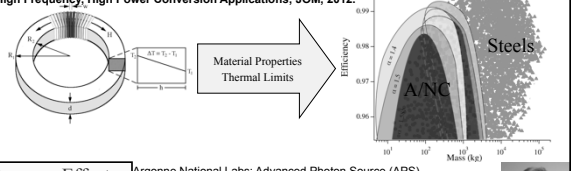

Pressure Effects

Argonne National Labs: Advanced Photon Source (APS)

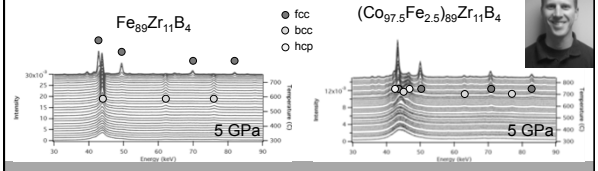

Nanocomposite Ribbons by Solid State Reactions

Amorphous and Nanocrystalline Materials for Applications as Soft Magnets. **M. E. McHenry**, M. A. Willard and D. E. Laughlin; *Prog. Mat. Sci.*, **44**, 291-433, (1999).

Why are Nanocomposite Magnets so "Soft"?

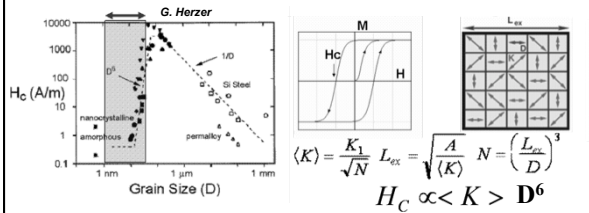

$$\langle K \rangle = \frac{K_1}{\sqrt{N}} \quad L_{ex} = \sqrt{\frac{A}{\langle K \rangle}} \quad N = \left(\frac{L_{ex}}{D}\right)^3$$

$$H_C \propto < K > \mathbf{D^6}$$

Energy loss upon cycling a magnetic material = Area of the hysteresis loop
Nanocrystalline Grains
→ **Strong Intergranular Exchange Interactions**
→ **Dramatic Reduction in Energy Losses**
High Resistivity of Nanocomposites Reduces Losses at High Frequency

Amorphous and Nanocrystalline Materials for Applications as Soft Magnets. **M. E. McHenry**, M. A. Willard and D. E. Laughlin; *Prog. Mat. Sci.*, **44**, 291-433, (1999).

Alloy Design

TL	TE	M	N
Fe	Ti V Cr	B C	Cu
Co	Zr Nb Mo	Al Si P	Ag
Ni	Hf Ta W	Ga Ge	Au

•**Primary crystallization** (diffusional)

TL = **Ferromagnetic TM's 85-90 at%**
TE = **Early TM glass former, growth inhibitor**
M = **Metalloid glass former**
N = **Noble Metal Nucleation Agent**
(unnecessary in HITPERM)
•**HITPERM is an Fe-Co based Nanocomposite Alloy**

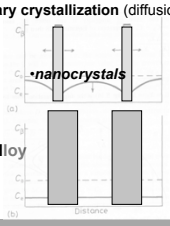

Structure and Magnetic Properties of $(Fe_xCo_{1-x})_yZr_zB_xCu_1$ Nanocrystalline Alloys. M. A. Willard, D. E. Laughlin, **M. E. McHenry**, D. Thoma, K. Sickafus, J. O. Cross and V. G. Harris, J. Appl. Phys. **84**, 6773-6775, (1998).

Results for Fe89Zr7B4 at 5 Gpa: Heating

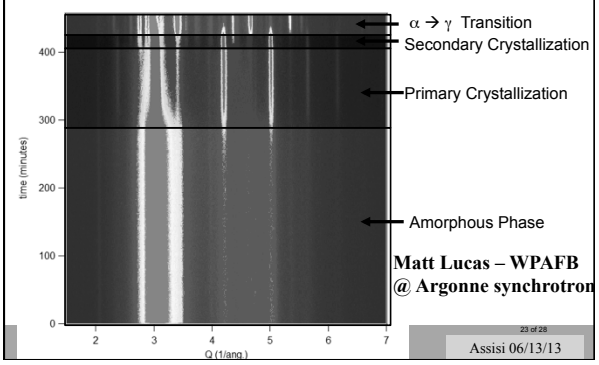

Matt Lucas – WPAFB
@ Argonne synchrotron

Near Equiatomic Fe-Co Alloys for Converters and Transformers.

Amorphous and Nanocrystalline Materials for Applications as Soft Magnets. **M. E. McHenry**, M. A. Willard and D. E. Laughlin; *Prog. Mat. Sci.*, **44**, 291-433, (1999).

Focal Area of Initial Research and Development

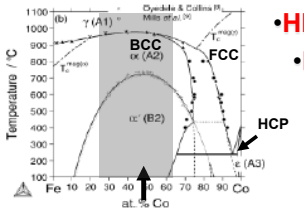

- **HITPERM Materials**
- **BCC nanox' tals**
- **Large B_s**
- **High T_C**
- **Large K_u**

Larger λ_s
More brittle

Despite tradeoffs we' ve demonstrated converter circuits with properties superior to FINEMET in an alloy with Magnetics, A Division of Spang & Co.

Induced Anisotropy in FeCo-based Nanocrystalline Ferromagnetic Alloys (HITPERM) by Very High Field Annealing. F. Johnson, H. Garmestani, S. Y. Chu, **M. E. McHenry** and D. E. Laughlin, IEEE Trans. Mag. **40**. 2724-2726 (2004).

Lab Scale

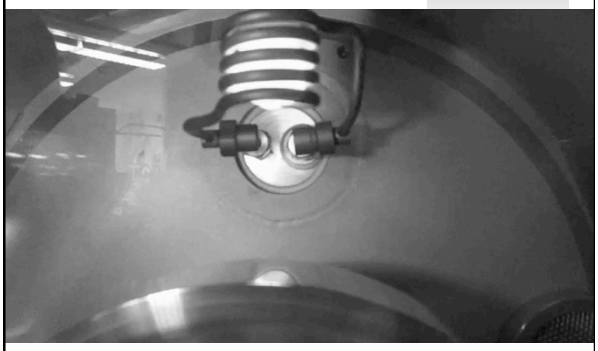

High Induction Materials for ARL Power Transformer

HTX002: $(Fe_{65}Co_{35})_{80+x}B_{13}Nb_{4-x}Si_2Cu_1$

- Ideal Fe:Co ratio of 65:35 found
- Nb-content reduced to increase induction
- 1 at% Nb alloy demonstrated low losses and high saturation induction.

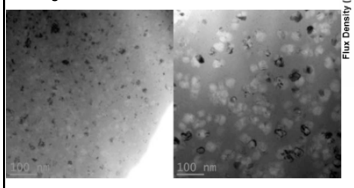

4 at% Nb **1 at% Nb**

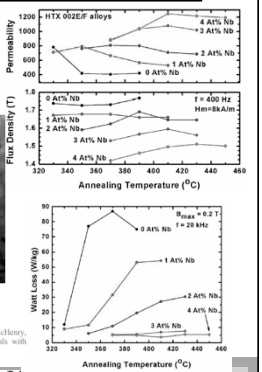

Kelsey J. Miller, Adam Wise, Alex Leary, David E Laughlin, Michael Edward McHenry, Vladimir Keylin, and Huth Joe. "Increased Induction in Nanocomposite Materials with Reduced Glass-Formers." *Journal of Applied Physics* 107, no. 9 (2010): 09A316-18.

Current FOM' s: Reduced Glass Formers

Permeabilty: 1200 Coercivity: < 20 A/m
Losses < 10 W/kG

Induction: 1.9 T lab, 1.7 T, Spang

20 kHz → 50 kHz
50 kHz → 100 kHz

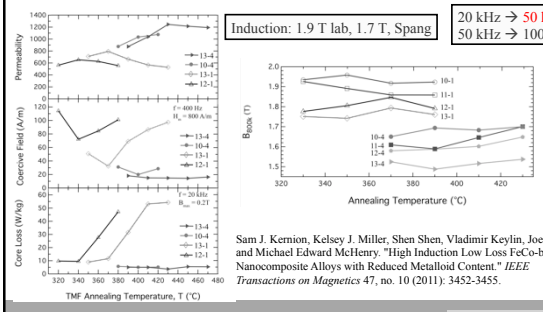

Sam J. Kernion, Kelsey J. Miller, Shen Shen, Vladimir Keylin, Joe Huth, and Michael Edward McHenry. "High Induction Low Loss FeCo-based Nanocomposite Alloys with Reduced Metalloid Content." *IEEE Transactions on Magnetics* 47, no. 10 (2011): 3452-3455.

FOM's: Polymorphous Primary & Secondary X'tallization

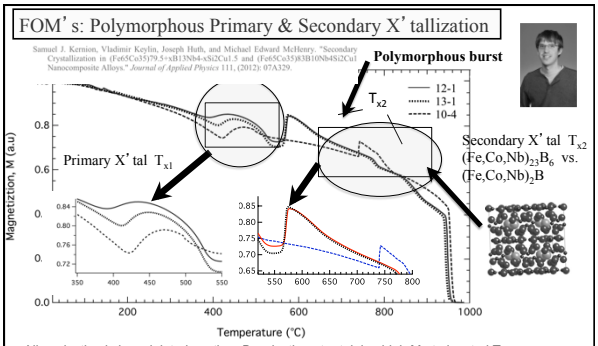

- Nb-reduction is less deleterious than B-reduction at retaining high M at elevated Ts
- M(T) of alloys with 1 at% Nb become level due to thick diffusion barrier, followed by early abrupt increase @T_{x2}
- 10-4 alloys display abrupt increase after slow diffusion.

Fe(Co)-B phase diagram on the Fe-rich end of the diagram and G(X) curves at T well below the eutectic and eutectoid T' s.

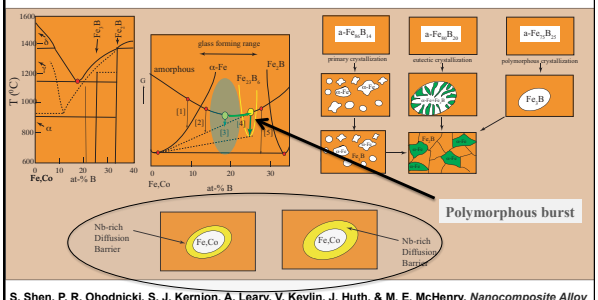

S. Shen, P. R. Ohodnicki, S. J. Kernion, A. Leary, V. Keylin, J. Huth, & M. E. McHenry. *Nanocomposite Alloy Design For High Frequency Power Conversion Applications.* Energy Technology 2012: Carbon Dioxide Management and Other Technologies, 265 (2012). TMS Warrendale, PA.

High Resitivity Alloys for Transformers.

S. Shen, S. J. Kernion, P. R. Ohodnicki and M. E. McHenry, Two-current Model of the Composition Dependence of Resistivity in Amorphous $(Fe_{100-x}Co_x)_{89-y}Zr_7B_4Cu_y$ Alloys Using a Rigid-band Assumption. J. Appl. Phys. 112, 103705 (2012).

Resistivity - I

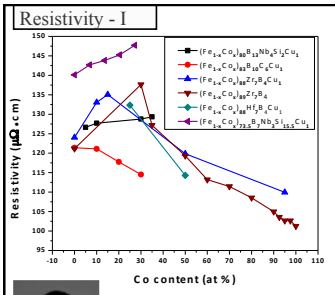

Additional data taken for Finemet with Co substitution and HITPERM with Hf

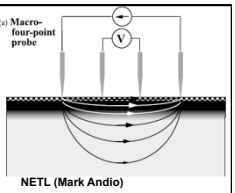

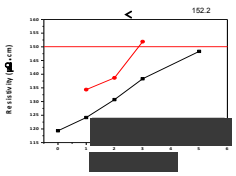

S. Shen, S. J. Kernion, P. R. Ohodnicki and M. E. McHenry, Two-current Model of the Composition Dependence of Resistivity in Amorphous $(Fe_{100-x}Co_x)_{89-y}Zr_7B_4Cu_y$ Alloys Using a Rigid-band Assumption. J. Appl. Phys. 112, 103705 (2012).

Resistivity

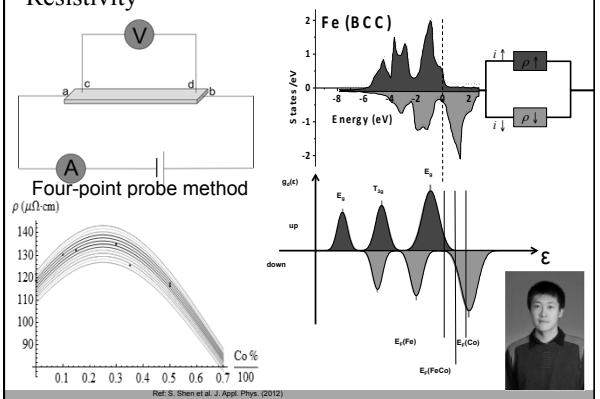

Ref: S. Shen et al. J. Appl. Phys. (2012)

←Exp. VBS Experiment Experiment→

Multiphase Resistivity Model

Equivalent Circuit of
-Series and
-Parallel paths for

1) **Amorphous,**
2) **Crystal, and**
3) **Shell Phases**

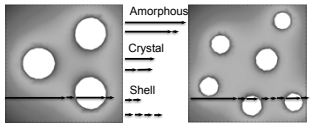

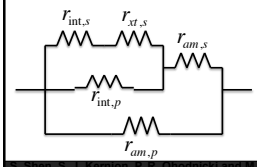

$$\frac{1}{r_{eq}} = \frac{1}{r_{am,p}} + \left(\left(\frac{1}{r_{am,s} + r_{xt,s}} + \frac{1}{r_{int,p}} \right)^{-1} + r_{am,s} \right)^{-1}$$

S. Shen, S. J. Kernion, P. R. Ohodnicki and M. E. McHenry, Two-current Model of the Composition Dependence of Resistivity in Amorphous $(Fe_{100-x}Co_x)_{89}Zr_7B_2Cu_2$ Alloys Using a Rigid-band Assumption. J. Appl. Phys. 112, 103705 (2012).

Process Scale-up.

Scale-Up

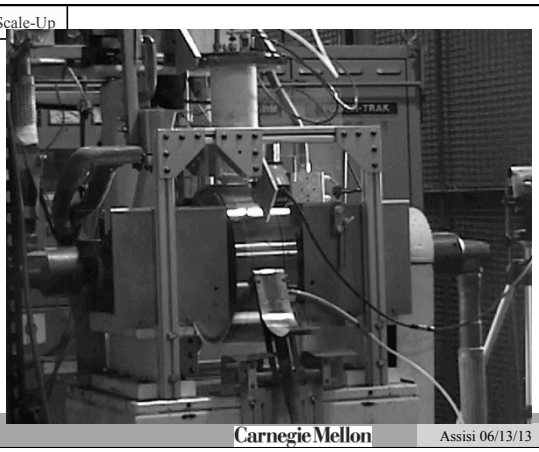

CMU Trials → Lab Caster Scale-up

Melt Spinning Processing

Planar Flow Casting

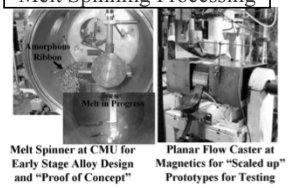

Melt Spinner at CMU for Early Stage Alloy Design and "Proof of Concept"

Planar Flow Caster at Magnetics for "Scaled up" Prototypes for Testing

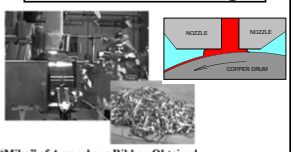

"Miles" of Amorphous Ribbon Obtained From Magnetics Planar Flow Cast

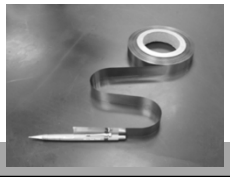

New High ρ Alloy Compositions
4 cm wide Ribbon
Reduced Thickness on Lab Caster
Improved Edge Integrity
Improved Surface Roughness

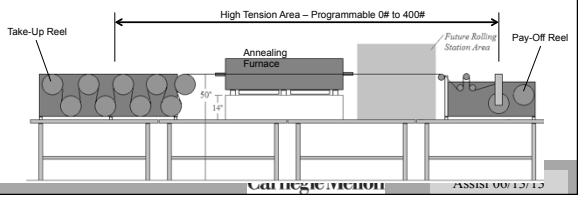

Joule Heating

- Joule heating experiments in air
- Limited oxide growth confirmed in SEM
- Heating rates ~100 K/sec
- Radiative heat loss dominates -> stable temperature control (ε = 0.3)
- Crystallization threshold determined by VSM, DSC, IR, and resistance

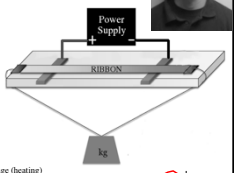

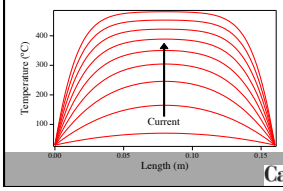

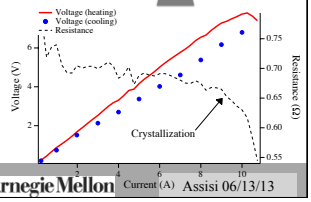

C-core Design, Graded Permeability, Higher Efficiency, Passive Cooling.

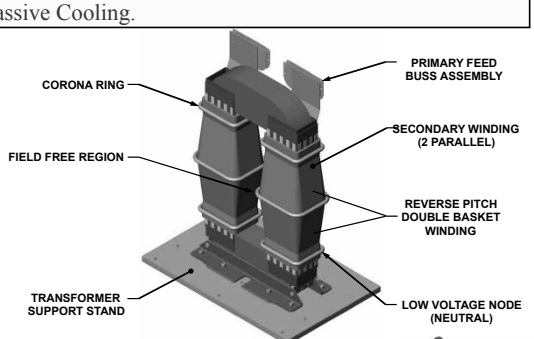

Advanced Winding Topology Minimizes Field Stresses and Leakage Inductance

Los Alamos NATIONAL LABORATORY

Crystallization, Phase Evolution and Chemical Partitioning in Co-rich Alloys.

- Co-rich alloys have lower B_s but high T_c
- $Fe_{1-x}Co_x$ has zero magnetostriction near x = 0.92
- Co-rich alloys have strong field annealing response.
- Co-rich alloys have superior corrosion resistance.
- Co-rich alloys have superior mechanical properties.
- Interesting physics in 2-,3- phase nanox'tallization processes.
- Alloys alos have large field tunable Giant Magnetoimpedance (GMI) Effect useful for current sensors.

Phase Evolution of Three-Phase Fcc, Hcp, and Amorphous Soft Magnetic Nanocomposite Alloy $Co_{88}Zr_7B_4$. P. R. Ohodnicki, H. McWilliams, D. E. Laughlin, M. E. McHenry, and V. Keylin, J. Appl. Phys. 103, 07E740, (2008).

Large Peak in K_U and Phase Evolution

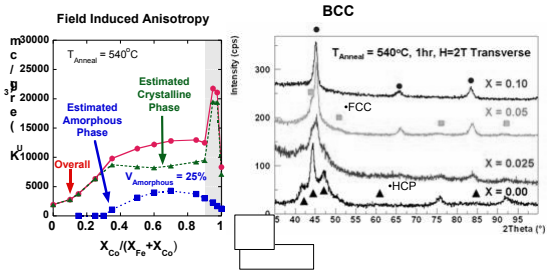

- Large K_U for Compositions with Multiple Crystalline Phases…

Co-rich Alloys

$(Co_{1-x}Fe_x)_{88}Zr_7B_4Cu$ $(Co_{0.96}Fe_{0.04})_{88}Zr_7B_4Cu_1$

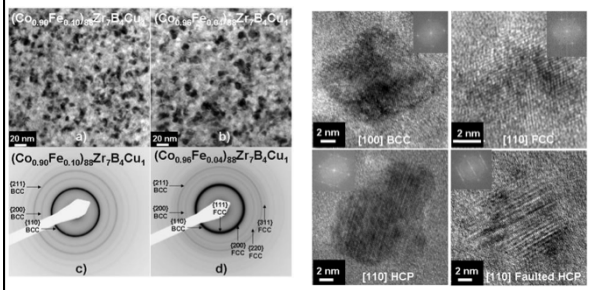

Only a BCC phase → x=0.10, 0.15
FCC phase → x=0.04

HCP phase w/ High Density of Stacking Faults for x=0.04

3DAP Study

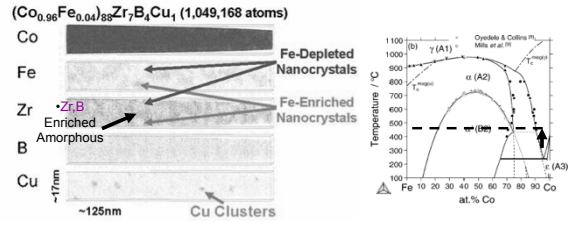

X = 0.04

3DAP Performed by K. Hono's Group at NIMS in Japan in Collaboration with M. Willard at NRL 3 Major Compositional Regions Identified in 3DAP Data.

Composition and Non-Equilibrium Crystallization in Partially Devitrified Co-rich Soft Magnetic Nanocomposite Alloys. P. R. Ohodnicki, Jr., Y. L. Qin, D. E. Laughlin, and M. E. McHenry, M. Kodzuka, T. Ohkubo, and K. Hono, M.A. Willard, Acta Mat. 57, 87-96, (2009).

T-stability of K_U -Longitudinal Field Reannealing

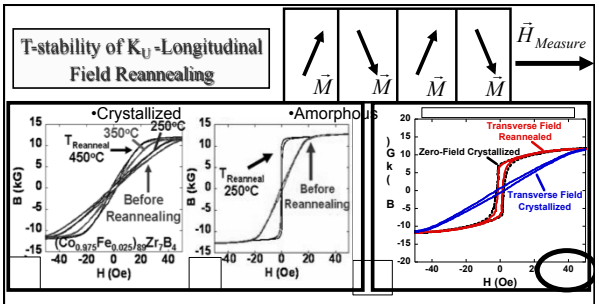

Field Crystallized Alloys Exhibit Higher T-Stability of H_K and K_U than Field Annealed Amorphous.

Maximum K_U Observed for Field X'tallization than Field Reannealing of Zero-Field Crystallized Ribbons.

Temperature Stability of Field Induced Anisotropy in Soft Ferromagnetic Fe,Co-Based Amorphous and Nanocomposite Ribbons. P. R. Ohodnicki, M. E. McHenry, and D. E. Laughlin, V. Keylin and J. Huth. *J. Appl. Phys.* 105, 07A322 (2009).

Experimental Procedure: EDXRD

Argonne NATIONAL LABORATORY HPCAT 16-BMB

Energy Dispersive X-Ray Diffraction

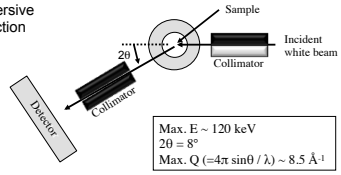

Max. E ~ 120 keV
2θ = 8°
Max. Q (=4π sinθ / λ) ~ 8.5 Å^{-1}

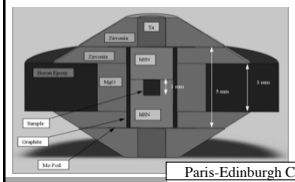

Paris-Edinburgh Cell

Hammer milled amorphous ribbon (100 × 30 μm)

Isochoric heating through Fe α→γ

Three pressures
0.5, 2.2, 4.9 GPa

Fixed 2θ = 8°

Pressure Effects on Microstructural Evolution

arpa·e Argonne NATIONAL LABORATORY

Wright-Patterson AFB

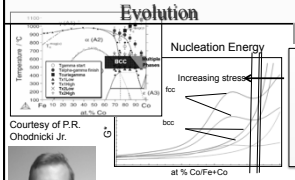

Courtesy of P.R. Ohodnicki Jr.

A. Leary, S. Kernion, M.A. Lucas, P. R. Ohodnicki, & M. E. McHenry, The Influence of Pressure on the Phase Stability of Nanocomposite $Fe_{88}Zr_7B_4Cu_1$ During Heating, accepted J. Appl. Phys. (2013).

Increase in primary crystallization T: Nanoperm: amorph → BCC +30 C at 5 GPa

Phase stabilization: Co-rich stabilizing close packed phases

Stuctural Evolution of Co-rich Nanocomposites at 5 GPa

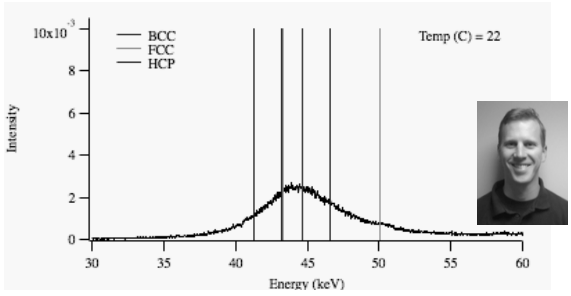

Inverse Magnetostricitve Effect: Loss Mechanisms

- **domain wall motion**
  - occurs if the magnetization vector is initially parallel to the applied field
  - domains with magnetization aligned in the direction of the applied field grow at the expense of domains aligned opposite of the direction of the applied field

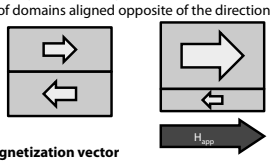

- **rotation of the magnetization vector**
  - occurs if the magnetization vector is initially perpendicular to the applied field
  - the magnetization vector rotates to align with the applied field
  - process is more reversible, typically results in less power loss

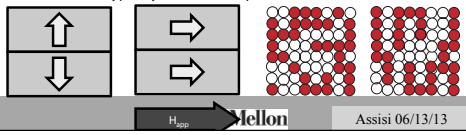

Strain Annealing in Fe-based Nanocomposites

- **Large Effect seen in Finemet - $Fe_{73.5}Si_{15.5}Nb_3B_7Cu_1$ (HTX-012)**
  - **Magneto-elastic effect again cited as cause of induced anisotropy.**
  - **Modeled by:**

$$K \approx -\frac{3}{2}\lambda_s^{FeSi}\sigma \bullet v_{cr}$$

  - **Residual strain seen in t-XRD experiments**
  - **Largest K_u = 130 kerg/cc (H_k = 260 Oe) seen in Finemet annealed with 780 MPa tension**

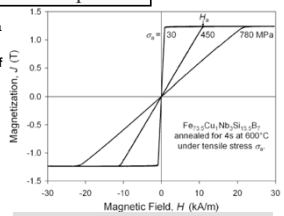

Herzer, G., Budinsky, V., & Polak, C. (2011). Journal of Physics: Conference Series, 266, 012010.

Negative λ

Applied Stress

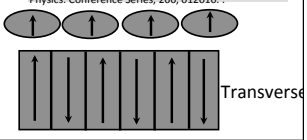

Methodology — Strain Annealing

Process – Ribbon Production

1)furnace is set to desired T

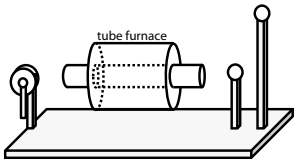

Methodology — Strain Annealing

Process – Ribbon Production

1) **furnace is set to desired temperature**
2) **amorphous magnetic ribbon is threaded through the setup; weight attached**
   - **weight supplies a constant tensile stress**
   - **pulleys facilitate ribbon's movement**

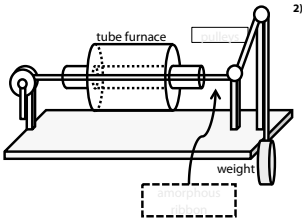

Methodology

Process – Ribbon Production

Strain Annealing

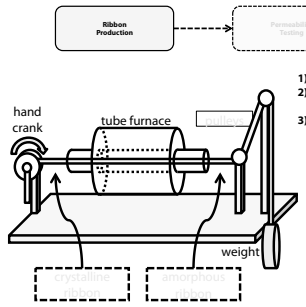

1) furnace is set to desired temperature
2) amorphous magnetic ribbon is threaded through the setup; weight attached
3) ribbon is delicately cranked through furnace using hand crank
   - as the amorphous ribbon passes through the effective heating area of the furnace, the ribbon crystallizes

Methodology

Process – Ribbon Production

Strain Annealing

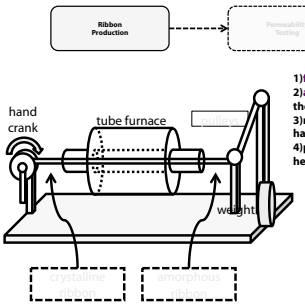

1)furnace is set to desired temperature
2)amorphous magnetic ribbon is threaded through the setup; weight attached
3)ribbon is delicately cranked through furnace using hand crank
4)process continued until weight reaches maximum height

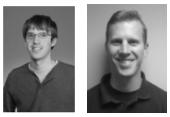

Strain Annealing in Fe-based HTX012 HTX003D

- 580°C, ~ 4 min effective annealing time. All loops at 1 kHz.
- Both HTX-012 and HTX-003D shows flattening of loop with strain annealing
- HTX-003D slightly higher induced anisotropy at higher stresses

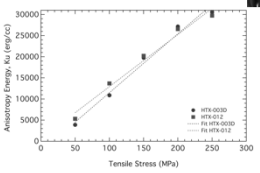

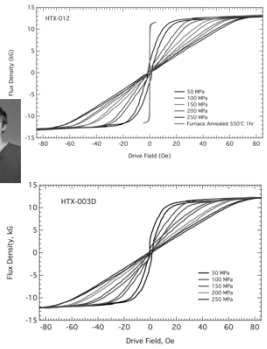

Strain Annealing in Co-rich Alloys

(H_k ~260 Oe @ 300MPa) !!

- Figure of Merit: Induced anisotropy per increment of stress

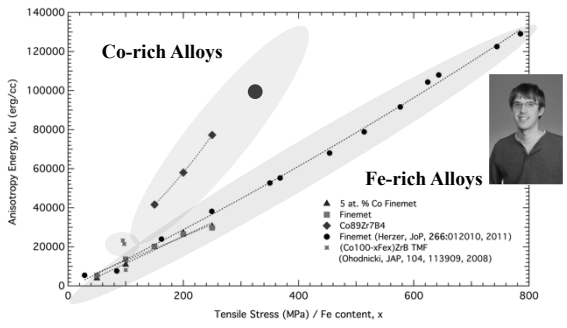

S. J. Kernion, A. Leary, S. Shen, J. Luo, J. Grossman, V. Keylin, J. F. Huth, M. S. Lucas, P. R. Ohodnicki, and M. E. McHenry; Giant Induced Magnetic Anisotropy in Strain-annealed Co-based Nanocomposite Alloys. Appl. Phys. Lett. 101, 102408-412 (2012); (http://dx.doi.org/10.1063/1.4751253).

Domains and Induced Anisotropy

Azuma et al., J. Appl. Phys. 111 (2012)

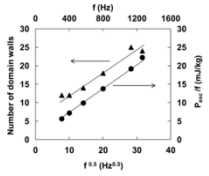

Flohrer et al., Acta Mat. 54 (2006)

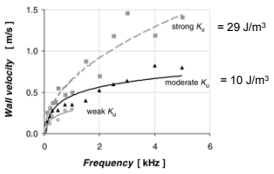

Higher f ⟶ faster walls ⟶ more domains

Higher K_u ⟶ wider domains ⟶ faster walls

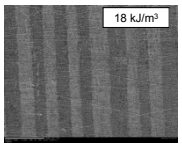

Deformation of Metallic Glasses

←Exp. Amorphous Experiment Experiment→

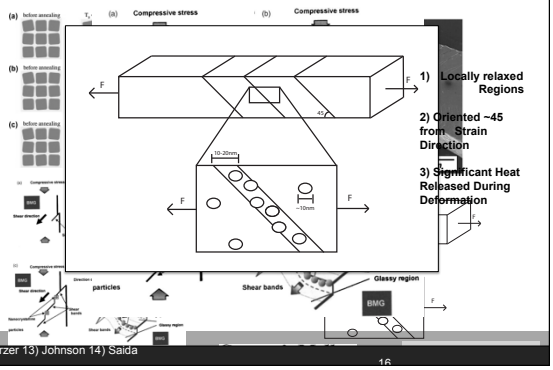

12) Herzer 13) Johnson 14) Saida

Conclusions

1. Magnetic nanocomposites contribute to applications including: Power conversion from renewable energy sources and for electric vehicles.
2. Progress is tied to synthesis → structure → properties relationships.
3. Power losses can be influenced by novel chemistries and processing to reduce thickness, increase resistivity, induce anisotropy so as to enable high frequency operation that can dramatically reduce the size and weight of power electronic components.
4. Power loss reductions allow for power conversion at frequencies in excess of 20 kHz and we hope in the near future (1-2 years) to demonstrate 100 kW – 1 MW power conversion.
5. Much remains to be done to further understand local structure and magnetic properties relationships.

Work in Progress

1. **Thickness reduction by mechanical rolling (WPAFB):**
   S. Kernion, M.A. Lucas, J. Horwath, Z. Turgut, E. Michel, V. Keylin, J. Huth, S. Shen, A. Leary and M. E. McHenry, Reduced Losses in FINEMET Nanocrystalline Ribbons. Abstract accepted MMM/Intermag 2013.
2. **Pressure effects on phase stability (APS/WPAFB):**
   A. Leary, S. Kernion, M.A. Lucas, P. R. Ohodnicki, and M. E. McHenry, The Influence of Pressure on the Phase Stability of Nanocomposite $Fe_{88}Zr_7B_4Cu_1$ During Heating Abstract accepted MMM/Intermag 2013.
3. **Amorphous phase viscosity and Induced Anisotropy.**
   A. Leary, J. Luo, S. Kernion, P. R. Ohodnicki, and M. E. McHenry. Impact of Structural Relaxation Events on Field Induced Anisotropy in Fe and Co-rich Amorphous Alloys. Abstract accepted MMM/Intermag 2013.
4. **Influencing Nucleation by Flash Annealing/Joule Heating.**
   CMU MSE Capstone Design Project.
5. **Magnetic Circular Dichroism Studies of Switching in Strain Annealed Samples.**

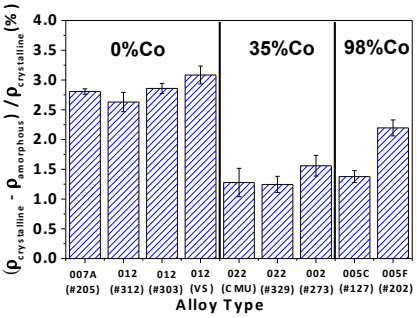

- Deviation of the amorphous density from corresponding crystalline density is more sensitive to Fe/Co ratio than manufacturing facility
- Fe-based alloys exhibited a larger deviation than alloys with Co content

Carnegie Mellon Assisi 06/13/13